First-principles study of phonons and superconductivity of $Nb_{1-x}Mo_x$ within the virtual-crystal approximation

2007 J. Phys.: Condens. Matter 19 476216

(http://iopscience.iop.org/0953-8984/19/47/476216)

IOP PUBLISHING JOURNAL OF PHYSICS: CONDENSED MATTER

J. Phys.: Condens. Matter **19** (2007) 476216 (8pp) doi:10.1088/0953-8984/19/47/476216

First-principles study of phonons and superconductivity of $Nb_{1-x}Mo_x$ within the virtual-crystal approximation

O De la Peña-Seaman[1,2], R de Coss[1], R Heid[2] and K P Bohnen[2]

[1] Departamento de Física Aplicada, Centro de Investigación y de Estudios Avanzados del IPN, Apartado Postal 73, Cordemex 97310 Mérida, Yucatán, Mexico
[2] Forschungszentrum Karlsruhe, Institut für Festkörperphysik, PO Box 3640, D-76021 Karlsruhe, Germany

E-mail: decoss@mda.cinvestav.mx and heid@ifp.fzk.de

Received 1 August 2007, in final form 1 August 2007
Published 5 November 2007
Online at stacks.iop.org/JPhysCM/19/476216

Abstract

We have studied the complete phonon dispersion, electron–phonon and superconducting properties of the $Nb_{1-x}Mo_x$ alloy within the framework of density functional perturbation theory using a mixed-basis pseudopotential method and the self-consistent virtual-crystal approximation. Complete phonon dispersions as a function of x were obtained in good agreement with experimental data, independent of the approximation used for the exchange–correlation functional. For the Eliashberg function $\alpha^2F(\omega)$ we found a shift of weight to higher frequencies as well as an overall reduction with increasing x up to $x \approx 0.7$; however, for $x = 1$ (pure Mo) the spectral weight for $\alpha^2F(\omega)$ increased again. We used the information of $\alpha^2F(\omega)$ to calculate and analyze the evolution of the average coupling strength $\lambda(x)$ and the superconducting temperature $T_c(x)$. The variation of $\lambda(x)$ closely follows the variation of the electronic density of states at E_F. For $T_c(x)$ experimental values were well reproduced provided a proper interpolation scheme for the Coulomb pseudopotential $\mu^*(x)$ was employed.

1. Introduction

The $Nb_{1-x}Mo_x$ alloy has been investigated extensively in the past because of its superconducting properties. In particular, the observation of the non-monotonic behavior of the superconducting critical temperature (T_c) as a function of Mo-content, x, has initiated numerous experimental and theoretical studies of its structural [1–5], electronic [6–12], vibrational [13–21], and superconducting properties [21–31]. While Nb possesses the highest T_c among elemental metals (9.25 K), T_c decreases with increasing Mo-content, falling below 0.5 K for $0.4 \leqslant x \leqslant 0.9$ and slightly recovering again to $T_c = 0.92$ K at $x = 1$ (Mo) [1, 22, 32].

The aim of this paper is to investigate the superconducting properties of this alloy system with modern *ab initio* density functional methods. This requires good knowledge of the electronic properties, a detailed microscopic description of the phonon dispersion as well as an accurate calculation of the electron–phonon coupling. Due to the presence of phonon anomalies in Nb and Mo as well as in the alloy system this is a non-trivial task.

Measurements of the phonon dispersions revealed a wealth of phonon anomalies which strongly depend on the value of x [13–15]. For example, on the one hand, Nb exhibits a Kohn anomaly in the longitudinal branch [00ζ], which is not present in Mo. On the other hand, in Mo there is a depression near the symmetry point H for the longitudinal and transverse branches [13–15]. The evolution of this anomaly in $Nb_{1-x}Mo_x$ was studied [15] using coherent one-phonon scattering of thermal neutrons and it was found that at $x \approx 0.4$ the anomaly starts to disappear, but for higher Mo concentrations ($x \geqslant 0.9$), a depression at the H-point appears suddenly. Another example is given by the transverse-mode frequencies at the N-point, where a reversal of the ordering is observed from Nb to Mo [15].

From the theoretical point of view non-stoichiometric systems add additional complications. To overcome these, different attempts have been made in the past to simulate the alloy by using quasirandom structures [4], the coherent potential approximation (CPA) [9–11], and the Korringa–Kohn–Rostoker coherent potential approximation (KKR-CPA) [12]. However, such studies have been limited to a few Mo concentrations, because these calculations are computationally very demanding, especially if one is interested in very low (close to Nb) or high concentrations (close to Mo). T_c was calculated only in a fairly global way by expressing the electron–phonon coupling λ as a function of x in terms of the Hopfield parameter (η) [12]. Combined with the Debye temperature and assumptions about the Coulomb pseudopotential μ^*, the general trend of $T_c(x)$ was reproduced with the McMillan formula [33]. Reliable quantitative values can only be obtained, however, from a more detailed treatment of the phonon dispersion and the electron–phonon coupling.

In this paper we present a study of complete phonon dispersions, electron–phonon and superconducting properties of the $Nb_{1-x}Mo_x$ alloy for eight different concentrations, $x = 0.0$, 0.1, 0.2, 0.3, 0.4, 0.5, 0.7, and 1.0, by combining density functional theory (DFT) [34] with the self-consistent virtual-crystal approximation (VCA) [35–37]. Vibrational properties as well as the electron–phonon coupling are obtained with the linear response theory [38–42]. Finally, superconductivity is discussed within the framework of the isotropic Eliashberg theory [43, 44]. We assess the accuracy of the VCA for describing complete phonon dispersion curves and superconducting properties of this alloy by comparison with available experimental data [13–15, 23–25, 27–29, 32].

2. Computational details

The present DFT calculations were performed with the mixed-basis pseudopotential method (MBPP) [45]. The $Nb_{1-x}Mo_x$ alloy was modeled in the self-consistent virtual-crystal approximation (VCA) [35, 36, 46–48]. For each x we generated a new pseudopotential with a fractional nuclear charge ($Z = 41 + x$). The valence charge is modified by the same amount in order to maintain the neutrality on the pseudo-atom. This approximation is possible since Mo and Nb are nearest neighbors in the periodic table. The potential for the VCA system is determined self-consistently for each value of x once we have constructed the pseudopotential. In a previous work [37], we verified the accuracy of the VCA implementation in the MBPP code, and found that this version of the VCA scheme works very reliably with respect to structural, electronic and phononic properties (for selected high-symmetry points at the Brillouin zone) of $Nb_{1-x}Mo_x$ for the full range of concentrations ($0 \leqslant x \leqslant 1$).

Details of pseudopotentials and basis functions can be found in our previous publication [37]. Phonon properties are accessed via density functional perturbation theory (DFPT) [38, 39] as implemented in the MBPP code [39, 41]. The calculations were carried out with two different approximations for the exchange–correlation functional, the local density approximation (LDA) using the Hedin–Lundqvist form [49] and the generalized gradient approximation (GGA) using the PBE functional [50–52]. The Brillouin-zone integration has been performed using Monkhorst–Pack special k-point sets with a Gaussian smearing of 0.2 eV and a grid of $32 \times 32 \times 32$. Complete spectra are obtained from a Fourier interpolation of dynamical matrices calculated on a $8 \times 8 \times 8$ q-point mesh. The same method also provides access to the screened electron–phonon matrix elements, which are the ingredients of the isotropic Eliashberg theory [43, 44]. All phonon calculations are based on full structural optimization for each x with respect to the total energy [37]. Finally, estimates for T_c are obtained via the Allen–Dynes formula [53].

3. Results and discussion

In figure 1 we display the phonon dispersions together with the corresponding phonon densities of states (PDOS) for varying Mo ($x = 0.0$, 0.1, 0.2, 0.3, 0.4, 0.5, 0.7, and 1.0). Results are shown for both xc-functionals, LDA and GGA and are compared with experimental data [15]. As a general trend, the phonon spectra harden with increasing x, which indicates a strengthening of the interatomic bonds from Nb to Mo. Comparing the two xc-functionals, GGA produces softer frequencies than LDA for all concentrations. However, both perform equally well with respect to experimental data for $x = 0.0$ and 0.4, with only a slight preference for LDA in the case of $x = 1$. With knowledge of the complete dispersion curves, we can now follow in more detail the evolution of the different anomalies present in $Nb_{1-x}Mo_x$ as a function of x, namely the Kohn anomaly at the Γ–H direction and the crossing of the transverse branches at the Γ–N direction. The latter is directly connected with the reordering of the transverse frequencies at the N-point mentioned above. We note that the Kohn anomaly becomes less deep as x grows and disappears for $x \approx 0.5$. In contrast, on the Mo side a strong softening occurs at the H-point. For the Γ–N direction the crossing of the transverse branches moves toward the zone boundary of ζ with increasing x until for $x \approx 0.5$ it reaches the N-point. For larger x the crossing disappears, while close to Mo, the lower transverse branch develops a depression in the vicinity of N.

We now discuss the electron–phonon coupling properties of the $Nb_{1-x}Mo_x$ alloy. In figure 2 we show our calculated electron–phonon spectral functions $\alpha^2F(\omega)$. With increasing x, the weight of the spectra is decreasing until $x \approx 0.7$, before recovering again for Mo. The shape of the spectra reflects the underlying PDOS, which explains the shift to higher frequencies when x increases, as well as the fact that the LDA spectra are always harder than the corresponding GGA ones.

Experimental information about $\alpha^2F(\omega)$ is only available for Nb. Results from various tunneling experiments [23–25, 29] are depicted in figure 2. While there is reasonable agreement for the low-frequency region, theory and experiments clearly differ with respect to the intensity of the high-frequency (longitudinal) peak. Theory predicts a significantly larger coupling of the longitudinal phonons than seen in all experiments. This discrepancy has also been found in previous calculations [21, 30, 43]. Early attempts to link it to difficulties related to the tunneling technique (e.g. preparation of high-quality junctions) have been falsified by extensive studies [23, 29]. This points to a currently unidentified shortcoming in the theoretical approach.

The spectral functions determine the electron–phonon mass enhancement parameter $\lambda(x)$ and the average effective frequency $\omega_{\log}(x)$. They are shown in figure 3 together with the density of states at the Fermi level $N(E_F)$. Both xc-functionals result in very similar $\lambda(x)$.

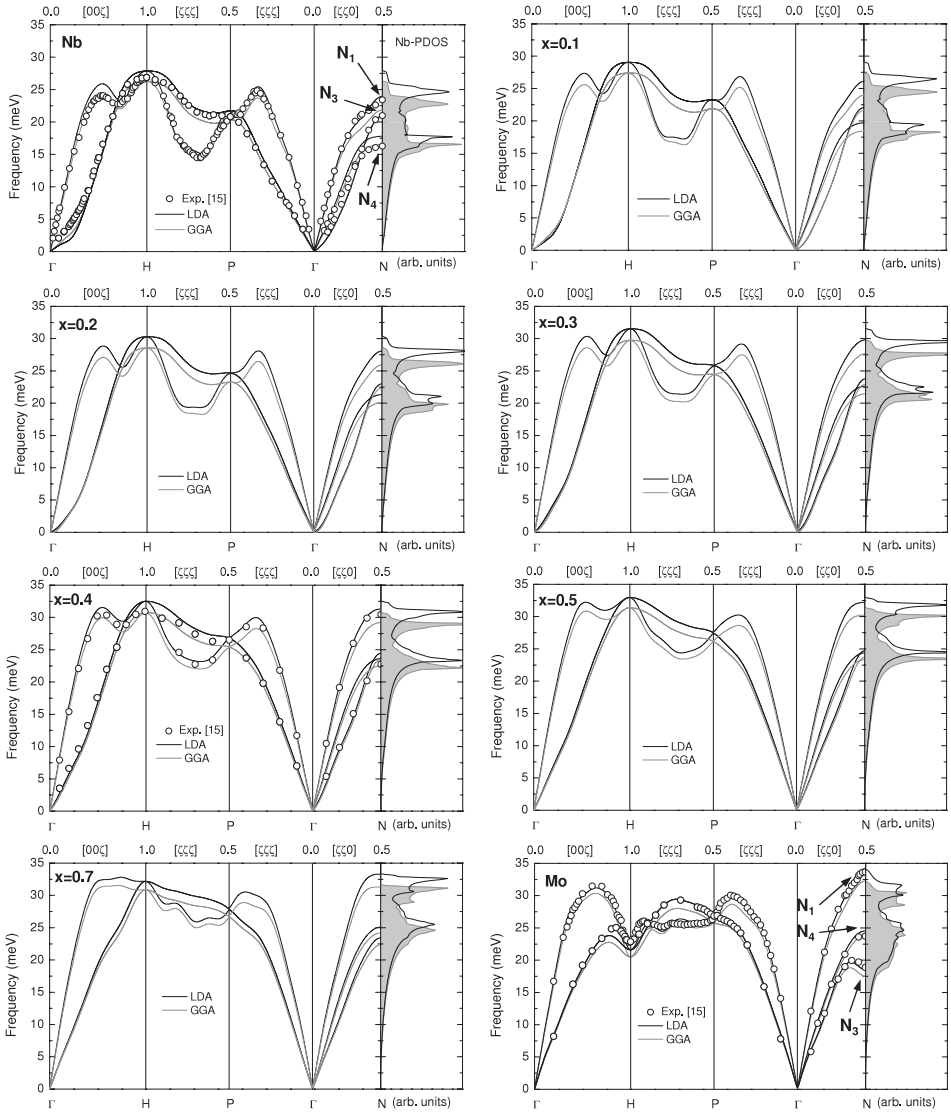

Figure 1. Calculated phonon dispersion curves and phonon density of states (PDOS) of $Nb_{1-x}Mo_x$ for eight concentrations using both xc-functionals. Measured data [15] are shown by empty circles.

At small x, λ decreases almost linearly until $x \approx 0.4$ and passes a shallow minimum in the range $0.4 \leqslant x \leqslant 0.7$ before increasing slightly toward $x = 1$ (Mo). A very similar behavior is exhibited by $N(E_F)$, which indicates that the variation of λ with x is predominantly determined by the variation of $N(E_F)$, and to a much lesser degree by the variation of the electron–phonon coupling. The effective phonon frequency entering the Allen–Dynes formula is always higher for LDA than for GGA, a feature that comes from the harder phonon spectrum for LDA. The increase of $\omega_{\log}(x)$ from Nb to Mo essentially occurs in the region $0.2 \leqslant x \leqslant 0.7$, while $\omega_{\log}(x)$ stays almost constant otherwise.

In comparison with previous theoretical work, our value of $\lambda = 0.41$ for Mo agrees very well with Savrasov *et al* ($\lambda = 0.42$) [21]. Similarly, for Nb, we obtain $\lambda \approx 1.33$, the same value

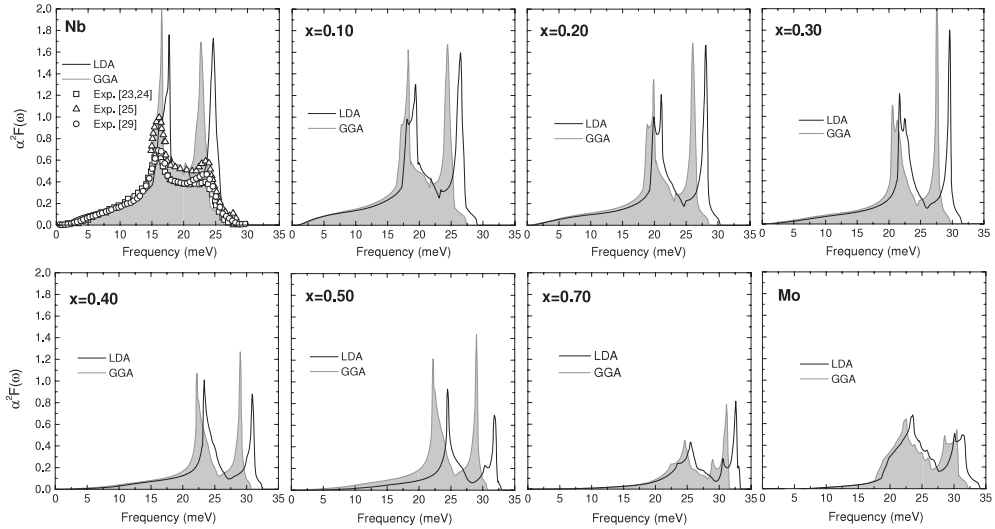

Figure 2. Calculated Eliashberg functions $\alpha^2 F(\omega)$ of $Nb_{1-x}Mo_x$ for both functionals, LDA and GGA. Symbols refer to spectra extracted from tunneling experiments [23–25, 29].

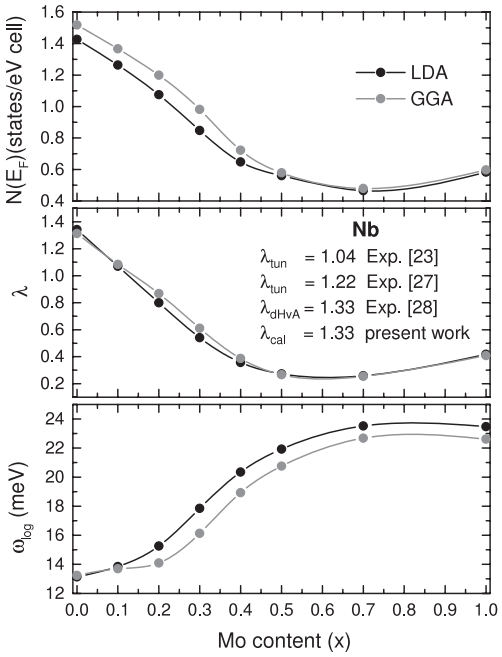

Figure 3. Evolution of $N(E_F)$, λ, and ω_{log} as a function of x for the $Nb_{1-x}Mo_x$ alloy.

found by Bauer *et al* [30]. A slightly smaller value was reported by Savrasov *et al* ($\lambda = 1.26$). This difference can be traced back to the use of the experimental lattice constant in the calculation of the electron–phonon coupling in the latter work, while in the present calculation, as well as those by Bauer *et al*, the theoretically optimized lattice constant was chosen. These theoretical values for λ (Nb) are of the order of 20% larger than those deduced from tunneling

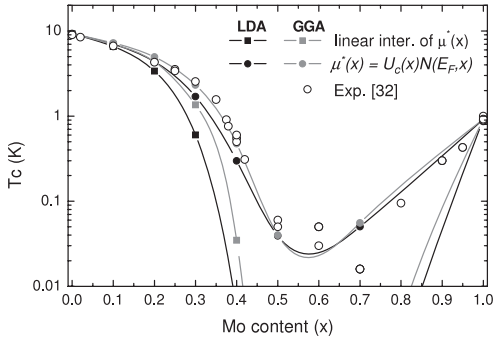

Figure 4. Calculated $T_c(x)$ on a logarithmic scale for $Nb_{1-x}Mo_x$ alloy using two different interpolation schemes for $\mu^*(x)$. For comparison, experimental data from [32] are shown as open symbols.

experiments (1.04 [23], 1.22 [27], 0.95–1.09 [29]), which is a direct consequence of the overestimation of the high-frequency part of the Eliashberg function discussed above. We note that, in contrast, from a de Haas–van Alphen [28] experiment a value of $\lambda = 1.33$ was extracted, in close agreement with theory.

For obtaining estimates of $T_c(x)$, we now apply the Allen–Dynes formula[3] [53]. Besides the quantities $\lambda(x)$ and $\omega_{\log}(x)$ discussed above, we require knowledge of μ^*, which is the only phenomenological parameter. We have considered two different interpolation schemes. The first one consists of a simple linear interpolation, $\mu^*(x) = \mu^*_{Nb}(1-x) + \mu^*_{Mo}x$, between the values of μ^* for Nb and Mo. The boundary values were chosen to fit the experimental T_c of 9.25 K for Nb and 0.92 K for Mo, giving $\mu^*_{Nb} = 0.224(0.219)$ and $\mu^*_{Mo} = 0.119(0.112)$ for LDA(GGA), respectively. Note that our μ^*_{Nb} is larger than the value from inversion of the tunneling data ($\mu^* \approx 0.15$–0.19 [29]). This is a consequence of the larger theoretical value of λ, and has been noted before by Savrasov *et al* [21]. The second scheme is based on the representation $\mu^*(x) = U_c(x)N(E_F, x)$ proposed by Gladstone *et al* [54]. Here we combine our calculated values for $N(E_F, x)$ with a linear interpolation of $U_c(x)$. The boundary values $U_c(\text{Nb}) = 0.158(0.144)$ and $U_c(\text{Mo}) = 0.205(0.188)$ for LDA(GGA), are again chosen to reproduce the T_cs of Nb and Mo, respectively.

In figure 4 we present the evolution of T_c as calculated with the two different interpolations of $\mu^*(x)$ for both LDA and GGA, and compare them with experimental data [32]. With both schemes, the experimental trend is well reproduced, that is, a reduction of T_c for smaller x, a minimum at $x \approx 0.5$–0.7, and then an increase toward Mo($x = 1$). The linear interpolation scheme performs poorly for intermediate values of x. A much improved description is obtained for the case of scaling of $\mu^*(x)$ with $N(E_F, x)$ for both xc-functionals, LDA and GGA, with a slightly better agreement for GGA in the region $x \leqslant 0.5$.

4. Conclusions

In summary, we have performed a first-principles study of complete phonon dispersions, electron–phonon and superconducting properties of the alloy series $Nb_{1-x}Mo_x$ as a function of x. In general we found very good agreement with experimental trends for all properties

[3] To check the accuracy of the Allen–Dynes formula in the strong coupling regime, we also solved the exact gap equation for the boundary cases of the alloy, Nb and Mo. The obtained differences in T_c of ≈3% and 5% for Nb and Mo, respectively, are negligible for the purpose of the present study.

investigated: (i) the hardening of the spectra with increasing x, and in particular the evolution of the various phonon anomalies, is well reproduced. Both LDA and GGA possess similar accuracy in describing the experimental phonon dispersions, although with LDA typically harder spectra are obtained. (ii) Following the behavior of the phonon density of states, the Eliashberg functions $\alpha^2 F(\omega)$ shift weight to higher frequencies with increasing x. Their total weight and the related coupling constant $\lambda(x)$ exhibit a non-monotonic behavior with a strong reduction at smaller x, a minimum at $x \approx 0.7$, and a slight increase toward $x = 1$ (Mo). The variation of the average coupling strength with x is to a large degree determined by the variation of the electronic density of states at the Fermi energy. Despite the differences in the phonon spectra, LDA and GGA predict almost the same $\lambda(x)$. (iii) The experimental $T_c(x)$ is well reproduced on the whole range of x, provided that the strong variation of $N(E_F, x)$ is properly incorporated in the interpolation of $\mu^*(x)$ as proposed by Gladstone *et al* [54]. The good agreement with experimental data indicates that the VCA provides an accurate approach to lattice dynamics and electron–phonon coupling properties of the alloy $Nb_{1-x}Mo_x$.

Acknowledgments

This research was supported by the Consejo Nacional de Ciencia y Tecnología (CONACYT, México) under grant no. 43830-F and the Forschungszentrum Karlsruhe, Germany. One of the authors, OP, gratefully acknowledges a student fellowship from CONACYT-México and the support from Forschungszentrum Karlsruhe.

References

[1] Goldschmidt H J and Brand J A 1961 *J. Less-Common Met.* **3** 44
[2] Catterall J A and Barker S M 1964 *Plansee Proc.* 577
[3] Hubbell W C and Brotzen F R 1972 *J. Appl. Phys.* **43** 3306
[4] Jiang C, Wolverton C, Sofo J, Chen L Q and Liu Z K 2004 *Phys. Rev.* B **69** 214202
[5] Bujard P, Sanjines R, Walker E, Ashkenazi J and Peter M 1981 *J. Phys. F: Met. Phys.* **11** 775
[6] Lomer W M 1962 *Proc. Phys. Soc. (London)* **80** 489
[7] Mattheiss L F 1965 *Phys. Rev.* **139** A1893
[8] Loucks T L 1965 *Phys. Rev.* **139** A1181
[9] Colavita E, Franciosi A, Rosei R, Sacchetti F, Giuliano E S, Ruggeri R and Lynch D W 1979 *Phys. Rev.* B **20** 4864
[10] Donato E, Ginatempo B, Giuliano E, Rugger R and Stancanell A 1982 *J. Phys. F: Met. Phys.* **12** 2309
[11] Bull C R, Kaiser J H, Alam A, Shiotani N and West R N 1984 *Phys. Rev.* B **29** 6378
[12] Rajput S S, Prasad R, Singru R M, Kaprzyk S and Bansil A 1996 *J. Phys.: Condens. Matter* **8** 2929
[13] Nakagawa Y and Woods A D B 1963 *Phys. Rev. Lett.* **11** 271
[14] Woods A D B and Powell B M 1965 *Phys. Rev. Lett.* **15** 778
[15] Powell B M, Martel P and Woods A D B 1968 *Phys. Rev.* **171** 727
[16] Varma C M and Weber W 1979 *Phys. Rev.* B **19** 6142
[17] Ho K M, Fu C L, Harmon B N, Weber W and Hamann D R 1982 *Phys. Rev. Lett.* **49** 673
[18] Zarestky J, Stassis C, Harmon B N, Ho K M and Fu C L 1983 *Phys. Rev.* B **28** 697
[19] Chen Y, Fu C L, Ho K M and Harmon B N 1985 *Phys. Rev.* B **31** 6775
[20] Singh D and Krakauer H 1991 *Phys. Rev.* B **43** 1441
[21] Savrasov S Y and Savrasov D Y 1996 *Phys. Rev.* B **54** 16487
[22] Hulm J and Blaugher R 1961 *Phys. Rev.* **123** 1569
[23] Wolf E L 1985 *Principles of Electronic Tunneling Spectroscopy* (New York: Oxford University Press)
[24] Arnold G B, Zasadzinski J and Wolf E L 1978 *Phys. Lett.* A **69** 136
[25] Wolf E L, Zasadzinski J, Osmun J W and Arnold G B 1980 *J. Low Temp. Phys.* **40** 19
[26] Bostock J, Diadiuk V, Cheung W N, Lo K H, Rose R M and MacVicar M L A 1976 *Phys. Rev. Lett.* **11** 603
[27] Bostock M J, MacVicar M L A, Arnold G B, Zasadzinki J and Wolf E L 1980 *Proc. 3rd Int. Conf. on Superconductivity of d- and f-Band Metals* ed H Suhl and M B Mapple (New York: Academic)

[28] Crabtree G W, Dye D H, Karim D P and Koelling D D 1979 *Phys. Rev. Lett.* **42** 390
[29] Geerk J, Gurvitch M, McWhan D B and Rowell J M 1982 *Physica* C **109** 1775
[30] Bauer R, Schmid A, Pavone P and Strauch D 1998 *Phys. Rev.* B **57** 11276
[31] Perlov C M and Fong C Y 1984 *Phys. Rev.* B **29** 1243
[32] *Landolt–Börnstein-Group III Condensed Matter* 1981 *Mo Based Alloys and Compounds* vol 21a (Heidelberg: Springer) and references therein
Landolt–Börnstein-Group III Condensed Matter 1981 *Nb–Mo, Nb Based Alloys and Compounds* vol 21b2 (Heidelberg: Springer) and references therein
[33] McMillan W L 1968 *Phys. Rev.* B **167** 331
[34] Kohn J W and Sham L J 1965 *Phys. Rev.* **140** A1133
[35] Mehl M J, Papaconstantopoulos D A and Singh D J 2001 *Phys. Rev.* B **64** 140509(R)
[36] De la Peña O, Aguayo A and de Coss R 2002 *Phys. Rev.* B **66** 012511
[37] De la Peña-Seaman O, de Coss R, Heid R and Bohnen K P 2007 *Phys. Rev.* B at press
[38] Louie S G, Ho K M and Cohen M L 1979 *Phys. Rev.* B **19** 1774
[39] Baroni S, Giannozzi P and Testa A 1987 *Phys. Rev. Lett.* **58** 1861
[40] Giannozzi P, de Gironcoli S, Pavone P and Baroni S 1991 *Phys. Rev.* B **43** 7231
[41] Heid R and Bohnen K P 1999 *Phys. Rev.* B **60** R3709
[42] Heid R, Bohnen K P and Ho K M 1999 *Phys. Rev.* B **57** 7407
[43] Savrasov S Y, Savrasov D Y and Andersen O K 1994 *Phys. Rev. Lett.* **72** 372
[44] Heid R, Pintschovius L, Reichardt W and Bohnen K P 2000 *Phys. Rev.* B **61** 12059
[45] Meyer B, Elsässer C and Fähnle M *FORTRAN90 Program for Mixed-Basis Pseudopotential Calculations for Crystals* (Stuttgart: Max-Planck-Institut für Metallforschung) unpublished
[46] Papaconstantopoulos D A, Economou E N, Klein B M and Boyer L L 1979 *Phys. Rev.* B **20** 177
[47] Ambrosch-Draxl C, Süle P, Auer H and Sherman E Y 2003 *Phys. Rev.* B **67** 100505(R)
[48] Thonhauser T and Ambrosch-Draxl C 2003 *Phys. Rev.* B **67** 134508
[49] Hedin L and Lundqvist B I 1971 *J. Phys. C: Solid State Phys.* **4** 2074
[50] Ozolins V and Korling M 1993 *Phys. Rev.* B **48** 18304
[51] Kokko K and Das M P 1998 *J. Phys.: Condens. Matter* **10** 1285
[52] Perdew J P, Burke K and Ernzerhof M 1996 *Phys. Rev. Lett.* **77** 3865
[53] Allen P B and Dynes R C 1975 *Phys. Rev.* B **12** 905
[54] Gladstone G, Jensen M A and Schrieffer J R 1969 *Superconductivity* vol 2, ed R D Parks (New York: Dekker)